

Definitive ideal-gas thermochemical functions of the H_2^{16}O molecule

Tibor Furtenbacher,¹ Tamás Szidarovszky,¹ Jan Hruby,² Aleksandra A. Kyuberis,³ Nikolai F. Zobov,³ Oleg L. Polyansky,⁴ Jonathan Tennyson,⁴ and Attila G. Császár*,¹

¹*MTA-ELTE Complex Chemical Systems Research Group, H-1117 Budapest, Pázmány Péter sétány 1/A, Hungary*

²*Department of Thermodynamics, Institute of Thermomechanics of the CAS, Dolejškova 5, Prague 8, CZ-18200, Czech Republic*

³*Institute of Applied Physics, Russian Academy of Science, Ulyanov Street 46, Nizhny Novgorod, Russia 603950*

⁴*Department of Physics and Astronomy, University College London, London WC1E 6BT, United Kingdom*

A much improved temperature-dependent ideal-gas internal partition function, $Q_{\text{int}}(T)$, of the H_2^{16}O molecule is reported for temperatures between 0 and 6000 K. Determination of $Q_{\text{int}}(T)$ is principally based on the direct summation technique involving all accurate experimental energy levels known for H_2^{16}O (almost 20 000 rovibrational energies including an almost complete list up to a relative energy of 7500 cm^{-1}), augmented with a less accurate but complete list of first-principles computed rovibrational energy levels up to the first dissociation limit, about $41\,000\text{ cm}^{-1}$ (the latter list includes close to one million bound rovibrational energy levels up to $J = 69$, where J is the rotational quantum number). Partition functions are developed for *ortho*- and *para*- H_2^{16}O as well as for their equilibrium mixture. Unbound rovibrational states above the first dissociation limit are considered using an approximate model treatment. The effect of the excited electronic states on the thermochemical functions is neglected, as their contribution to the thermochemical functions is negligible even at the highest temperatures considered. Based on the high-accuracy $Q_{\text{int}}(T)$ and its first two moments, definitive results, in 1 K increments, are obtained for the following thermochemical functions: Gibbs energy, standardized enthalpy, entropy, and isobaric heat capacity. Reliable approximately two standard deviation uncertainties, as a function of temperature, are estimated for each quantity determined. These uncertainties emphasize that the present results are the most accurate ideal-gas thermochemical functions ever produced for H_2^{16}O . It is recommended that the new value determined for the standard molar enthalpy increment at 298.15 K, $9.90404 \pm 0.00001\text{ kJ mol}^{-1}$, should replace the old CODATA datum, $9.905 \pm 0.005\text{ kJ mol}^{-1}$.

Keywords: bound and unbound states; ideal-gas thermochemical quantities; nuclear motion theory; *ortho*- and *para*- H_2^{16}O ; partition function; water

Contents

List of Tables	2
List of Figures	3
1. Introduction	4
2. Methodological Details	7
2.1. MARVEL energy levels	7
2.2. First-principles energy levels	8
2.3. The hybrid database	8
2.4. Thermochemical quantities	9
2.5. The effect of unbound states on the thermochemical properties of water	10
2.6. Uncertainty and error analysis	11
3. Results and Discussion	18
3.1. The partition function	19
3.2. Comparison with previous results	19
3.3. NASA polynomials	20
3.4. CODATA	21
3.5. The low-temperature limit	22
4. Summary and Conclusions	23
Acknowledgments	25
References	25

List of Tables

1	Physical constants employed in this study.	8
2	The temperature-dependent internal partition functions of <i>ortho</i> - and <i>para</i> - H_2^{16}O , $Q_{\text{int}}^{\text{ortho}}(T)$ and $Q_{\text{int}}^{\text{para}}(T)$, respectively, and their first two moments, Q' and Q'' . The same data are also presented for the nuclear-spin-equilibrated quantity $Q_{\text{int}}(T)$. Numbers in parentheses are the approximate two standard deviation uncertainties in the last digits of the $Q_{\text{int}}(T)$, $Q'_{\text{int}}(T)$, and $Q''_{\text{int}}(T)$ data.	16
3	Thermochemical functions of nuclear-spin-equilibrated H_2^{16}O . Numbers in parentheses are the approximate two standard deviation uncertainties in the last digit of the quoted value.	17
4	Coefficients of the fit, see Eq. (17), to the nuclear-spin-equilibrated internal partition function of H_2^{16}O	19

List of Figures

1	Left panel: Convergence of the internal partition function $Q_{\text{int}}(T)$ of H_2^{16}O at different temperatures as a function of the energy cutoff value considered in the direct sum (see text). Right panel: Similar curves for the isobaric heat capacity $C_p(T)$ of H_2^{16}O	12
2	Left panel: Convergence characteristics of the internal partition function, $Q_{\text{int}}(T)$ (solid lines), and the second moment of $Q_{\text{int}}(T)$, $Q''_{\text{int}}(T)$ (dashed lines), of H_2^{16}O utilizing larger and larger sets of energy levels, as a function of temperature, with energy cutoff values given in the inset of the figure. Right panel: Similar curves for the isobaric heat capacity $C_p(T)$ of H_2^{16}O	14
3	Error of the partition function (solid lines) and its second moment (dashed lines) using the propagation formula method, Method A, and the “two extrema” method, Method B.	14
4	Error due to the neglect of the unbound states during the determination of $Q''_{\text{int}}(T)$ (solid line) and $C_p(T)$ (dashed line).	15
5	Error contribution of energy levels (solid lines) and the error contribution of the uncertainty of second radiation constant (dashed lines).	18
6	Percentage difference between the “exact” values of $Q_{\text{int}}(T)$ and $C_p(T)$ and those corresponding to the “analytical” rigid-rotor–harmonic-oscillator (RRHO) approximation. The apparent increase in the differences below 350 K for $Q_{\text{int}}(T)$ is due to the failure of approximating the direct sum with an integral when the density of states is low.	20
7	Left panel: Comparison of the present $Q_{\text{int}}(T)$ values with those of Harris <i>et al.</i> , ²⁹ Irwin, ⁶⁶ and Vidler and Tennyson. ³⁰ Right panel: Comparison of the present $C_p(T)$ values with those of Harris <i>et al.</i> , ²⁹ JANAF, ¹⁵ and Vidler and Tennyson. ³⁰	21
8	The <i>ortho</i> - H_2^{16}O (dotted, blue curve), the <i>para</i> - H_2^{16}O (dashed, red curve), and the nuclear-spin-equilibrated H_2^{16}O (full, black curve) partition functions at low temperatures, below 50 K.	22
9	The <i>ortho</i> - H_2^{16}O (dotted, blue curve), the <i>para</i> - H_2^{16}O (dashed, red curve), and the nuclear-spin-equilibrated H_2^{16}O (full, black curve) isobaric heat capacities at low temperatures, below 100 K.	23

1. Introduction

Water, the most abundant polyatomic molecule in the universe, plays a major role in the radiative balance of the atmospheres of many astronomical objects, including the atmosphere of our own earth.^{1–3} Water is ubiquitous in cool stellar and substellar (brown dwarf) environments where it is present over a wide range of temperatures including very high ones ($T > 3000$ K), outside the range of most experimental laboratory techniques. Water is also important for models of combustion systems^{4,5} at medium to high temperatures (though still less than 3000 K). Predicting high-temperature thermochemical quantities and high-temperature spectra of water is important for understanding many of these environments. The related modeling studies need the accurate knowledge of the partition function, $Q(T)$, of water from the cold to the hot and some other ideal-gas thermochemical functions which can be determined straightforwardly⁶ from $Q(T)$.

Due to their considerable scientific and engineering interest, temperature-dependent thermochemical properties of molecular systems such as water have been reported in several databases and information systems.^{5,7–19} Most useful for many practical applications would be real-gas and not ideal-gas data,¹⁹ but these are available only for a relatively small number of molecules and they are hard to obtain via theoretical (quantum chemical) approaches. Ideal-gas data, forming the majority of data in the cited information systems, are considerably more straightforward to obtain theoretically. As emphasized in standard textbooks,^{6,20,21} all ideal-gas temperature-dependent thermochemical functions can be derived from the partition function and its moments. It would be preferable to obtain accurate temperature-dependent thermochemical functions experimentally. However, even in the few cases and temperature ranges where this is available it is built upon effective (anharmonic) spectroscopic quantities, which puts a considerable constraint on the accuracy that can be expected from such studies, especially at elevated temperatures. To accommodate the full temperature range required by the applications, one must rely on some sort of computation in order to derive the ideal-gas partition and thermochemical functions.

It is important to point out that ideal-gas thermochemistry has been developed with an emphasis on chemical reactions; thus, only those effects have been considered important which readily change during a chemical reaction. A consequence, as noted by Ruscic,¹⁹ is that “practical *thermochemical* functions ignore the overall nuclear spin contribution... as well as the isotope mixing component, which, in any stoichiometrically balanced chemical reaction, cancel out across the involved chemical species.” In spectroscopy, in scientific and engineering applications requiring line-by-line data, and when treating systems out of equilibrium (see, *e.g.*, Ref. 22), partition functions and thermochemical functions containing nuclear-spin contributions may be needed. Thus, in this paper we do consider nuclear spins in our treatment and compute thermochemical quantities for *ortho*- and *para*-H₂¹⁶O, as well as

for their nuclear-spin-equilibrated mixture. Treatment of the state-independent degeneracy factor is made simple here by the fact that the non-permuting ^{16}O nucleus has zero nuclear spin.

For many semirigid molecules, the simplest analytic technique^{21,23} to obtain internal partition functions, namely use of the harmonic oscillator (HO) and rigid rotor (RR) approximations for the vibrational and the rotational motions, respectively, yield reasonably accurate results at relatively low temperatures (especially around room temperature). Partition functions have an integrative nature: basically they are a direct sum of weighted energy levels. This provides much room for approximate treatments; for example, an approach more sophisticated than the RRHO approximation uses effective spectroscopic Hamiltonians providing a much improved estimate for the partition functions and the related thermochemical data, even up to somewhat elevated temperatures.^{24–26} For water, the perturbative approach is insufficient and even breaks down at relatively low excitations or, alternatively, at relatively low temperatures. Therefore, to obtain highly accurate, high-temperature partition and thermodynamic functions for the water isotopologues requires the use of variational techniques during the computation of the energy levels.²⁷

A considerable volume of knowledge has been accumulated about computing thermochemical functions for H_2^{16}O . Important developments on the computational front include studies by Martin *et al.*,²⁸ Harris *et al.*,²⁹ Vidler and Tennyson (VT),³⁰ and others.^{19,31–33} Two major sources of high-quality thermochemical data are JANAF (Joint Army-Navy-Air Force)¹⁵ and Gurvich,^{11,34} which were originally set up to supply, after appropriate compilation and evaluation, thermochemical data for modeling the thermochemistry of a large number of small and medium-sized chemical systems. For the presentation of the results of this study, the JANAF standard is followed: the JANAF-style tables list energy functions, entropies, enthalpies, and heat capacities as a function of temperature up to 6000 K. The JANAF tables themselves list thermochemical functions from 100 K with 100 K increments, but in the present study, due to the high experimental spectroscopic accuracy of our lower energy levels, we can list meaningful thermochemical quantities at even lower temperatures. Furthermore, in the Supplementary Material³⁵ to this paper the thermochemical quantities are listed at 1 K intervals to ensure that future interpolation efforts could retain the high accuracy of the present study. Furthermore, the International Association for the Properties of Water and Steam (IAPWS),¹⁶ an expected user of the data supplied here, requires thermodynamic data tabulated with this fine granularity.

Our data, with the associated approximately two standard deviation uncertainties, should be considered as the most accurate ideal-gas thermochemical data available for H_2^{16}O . There are several facets of the present study supporting this statement. Prior to the PoKaZaTeL data³⁶ used in the present study (*vide infra*), the most complete *ab initio* database for H_2^{16}O energy levels and transitions was the so-called BT2 line list,³⁷ which contains 221 097

energy levels (up to $J = 50$ and $E \leq 30\,000\text{ cm}^{-1}$) and half a billion transitions. The high-accuracy first-principles PoKaZaTeL dataset employed in this study is complete up to the first dissociation limit and contains four times more, close to one million energy levels. Prior to the present work, the most reliable partition sum and related thermochemical data was due to VT.³⁰ VT used a hybrid approach similar to the one employed here, but one which was necessarily more approximate. They summed over the then available empirical energy levels,³⁸ augmented with levels from a variational line list computed by Viti,^{39,40} and then completed it with predicted band origins to dissociation⁴¹ combined with a very approximate treatment of rotation. All sums were simply truncated at the dissociation limit which was assumed to be $41\,088\text{ cm}^{-1}$; any states lying above this limit were ignored. The present study utilizes a much larger set of experimental energy levels and a much larger set of computed first-principles energy levels than any of the previous studies.

Due to the Boltzmann distribution characterizing thermodynamic equilibria, the contribution of energy levels to the partition function depends strongly on the thermodynamic temperature T of the system. At the lowest temperatures, where the thermochemical functions depend only on a relatively small number of energy levels, an accuracy considerably higher than that provided by even the most sophisticated modeling studies can be achieved, once energy levels of experimental quality are used. At the lowest temperatures, one must also be careful how the *ortho* and *para* nuclear-spin isomers of H_2^{16}O are treated.²² These isomers are treated explicitly during the present study.

Given the high accuracy we aim at in this study up to very high temperatures, one must investigate not only the contribution of bound rovibrational states on the ground electronic state to the thermochemical functions, but also those of resonance states and higher electronic states. As shown recently for the case of three isotopologues of the diatomic molecule MgH ,⁴² beyond a given temperature, dependent upon the first dissociation threshold of the molecule, unbound states can make a significant contribution to the partition function and the related thermochemical quantities. Studies have begun to consider quasibound states of water,^{43,44} and in this paper such molecular states are considered for the partition function of water for the first time, albeit via a very simple model.

In a complete treatment, the contribution of excited electronic states must also be investigated. The effect of the excited electronic states of H_2^{16}O has not been considered during the present study, as it deemed to be minuscule even at the high accuracy sought in this study.

Finally, we note that many of the modeling methods of the present investigation on H_2^{16}O can be utilized when determining temperature-dependent thermochemical functions of other molecular systems.

2. Methodological Details

The total partition function is assumed to be the product of the internal and the translational partition functions. The bound rovibrational energy levels used for computing the ideal-gas internal partition function, $Q_{\text{int}}(T)$, of H_2^{16}O come from two sources: a Measured Active Rotational-Vibrational Energy Levels (MARVEL)^{45–47} analysis of all the available experimental transitions,⁴⁸ and a recent first-principles computation, utilizing the PoKaZaTeL potential energy surface (PES),³⁶ of all the bound rovibrational states on the ground electronic state of H_2^{16}O . These two sources will be described separately, followed by a discussion of the computation of the thermochemical functions. Since it is important to understand the accuracy of all the computed thermochemical quantities, an error and uncertainty analysis is also performed as part of this section.

2.1. MARVEL energy levels

The most accurate source of bound rovibrational energy levels of H_2^{16}O is the MARVEL database, obtained as part of an IUPAC-sponsored research effort.^{48–52} The MARVEL process⁴⁶ involves a weighted least-squares algorithm, whereby first a spectroscopic network (SN)⁵³ is built from the experimentally observed and assigned (labelled) spectral transitions, involving all available sources of data, and then the transitions, based on the Ritz principle, are inverted to determine experimental-quality (MARVEL) energy levels. Each transition has a label for the upper and lower states between which the transition occurs. The labeling scheme for H_2^{16}O uses six quantum numbers: the approximate normal-mode quantum numbers v_1 , v_2 , and v_3 describe the vibrations (symmetric stretch, bend, and anti-symmetric stretch, respectively), and the usual exact J rotational quantum number and the approximate K_a and K_c values are used for the description of the rotational excitation.⁵⁴

The MARVEL database⁴⁸ for H_2^{16}O contains 18 486 energy levels, all the known and validated experimentally determined bound rotational-vibrational energy levels of H_2^{16}O prior to 2013. The uncertainty of the MARVEL energy levels is between 10^{-6} and 10^{-2} cm^{-1} ; each energy level carries its own uncertainty. Even with the MARVEL database at hand, complete in rovibrational energies up to about 7500 cm^{-1} , one must realize that for higher temperatures (above about 600 K) there are insufficient observed rovibrational energy levels available to converge the partition function of H_2^{16}O to 10^{-4} % accuracy, the characteristic accuracy below 600 K. Therefore, if accurate thermochemical functions are needed at higher temperatures one must substantially augment the experimental (MARVEL) set of rovibrational energy levels. In the fourth age of quantum chemistry,⁵⁵ the best way to achieve this is through the use of results from first-principles nuclear motion computations, employing an exact nuclear kinetic energy operator and a highly accurate adiabatic global PES.⁵⁶

2.2. First-principles energy levels

Following this recommendation, in this study the MARVEL energy levels are augmented for the bound states by first-principles energy levels. The first-principles bound rovibrational energy levels used during this study are taken from a database called PoKaZaTeL.³⁶

The PoKaZaTeL energy levels were computed using a global, adiabatic, empirically adjusted PES³⁶ and the DVR3D nuclear-motion code.⁵⁷ This data set contains 810 252 energy levels up to the first dissociation limit ($D_0 = 41\,145.94(12)\text{ cm}^{-1}$),⁵⁸ and it extends all the way to $J = 69$. As a result, the PoKaZaTeL set represents all the bound rovibrational energy levels of H_2^{16}O .

2.3. The hybrid database

The most accurate and most complete database of bound rovibrational energy levels of H_2^{16}O can be obtained by combining the complete PoKaZaTeL database with the accurate MARVEL database. Therefore, we replaced the PoKaZaTeL energy levels with MARVEL energies whenever possible and in this way we obtain what is called hereafter the hybrid database.

For quantification of the approximately two standard deviation uncertainties of the computed thermochemical quantities, it is essential that each energy level has its own uncertainty. The experimental MARVEL energy levels have well determined uncertainties, originating from the uncertainties of the measured transitions. The computed PoKaZaTeL list does not have associated uncertainties. However, by comparing the PoKaZaTeL and MARVEL energy levels, when both are available, we could estimate the average uncertainties of the PoKaZaTeL energy levels. Finally, up to $20\,000\text{ cm}^{-1}$ a value 0.2 cm^{-1} was taken for these one standard deviation uncertainties, while above this energy a conservative estimate of 0.5 cm^{-1} was assumed.

Table 1. Physical constants employed in this study.

Name	Value	Reference
Second radiation constant, c_2	$1.43877736(83)\text{ cm K}$	59
Molar gas constant, R	$8.3144598(48)\text{ J mol}^{-1}\text{ K}^{-1}$	59
Avogadro constant, N_A	$6.022\,140\,857(74) \times 10^{23}\text{ mol}^{-1}$	59
Planck constant, h	$6.626070040(81) \times 10^{-34}\text{ J s}$	59
Boltzmann constant, k_B	$1.38064852(79) \times 10^{-23}\text{ J K}^{-1}$	59
H_2^{16}O molecular mass, m	$2.990724580(36) \times 10^{-26}\text{ kg}$	60

2.4. Thermochemical quantities

The internal partition function of a free molecule, Q_{int} , and its first two moments, Q'_{int} and Q''_{int} , can be written as^{6,28,33}

$$Q_{\text{int}} = \sum_i g_i (2J_i + 1) \exp\left(\frac{-c_2 E_i}{T}\right), \quad (1)$$

$$Q'_{\text{int}} = \sum_i g_i (2J_i + 1) \left(\frac{c_2 E_i}{T}\right) \exp\left(\frac{-c_2 E_i}{T}\right), \quad (2)$$

$$Q''_{\text{int}} = \sum_i g_i (2J_i + 1) \left(\frac{c_2 E_i}{T}\right)^2 \exp\left(\frac{-c_2 E_i}{T}\right), \quad (3)$$

where $c_2 = hc/k_{\text{B}}$ is the second radiation constant (the numerical values of the constants employed in this study are given in Table 1), J_i is the rotational quantum number, E_i is the rotational-vibrational energy level given in cm^{-1} , T is the thermodynamic temperature in K, g_i is the nuclear spin degeneracy factor (representing both state-dependent and state-independent elements), and the index i runs over all possible rovibronic energies considered. In the case of H_2^{16}O , the values of g_i are taken as 3 for the *ortho* and 1 for the *para* nuclear-spin states, in accord with the HITRAN convention.¹⁷

The full partition function Q of a molecule in the ideal gas state is a product of the internal partition function, Q_{int} , and the translational partition function, Q_{trans} . The latter can be expressed as²¹

$$Q_{\text{trans}} = V \Lambda^{-3}, \quad (4)$$

where V is the volume of the system, $\Lambda = h/(2\pi m k_{\text{B}} T)^{1/2}$ is the de Broglie wavelength, h is the Planck constant, and m is the molecular mass (the numerical values of the constants are given in Table 1).

The Helmholtz energy A , the internal energy minus the product of thermodynamic temperature and entropy, is obtained from its fundamental relation to the canonical partition function Q , namely

$$A = -RT \ln Q = -RT \ln Q_{\text{int}} - RT \ln \frac{V}{\Lambda^3}, \quad (5)$$

where R denotes the molar gas constant (Table 1). All thermochemical functions can then be derived using thermodynamic identities; in particular,

$$p = -\frac{\partial A}{\partial V}, \quad S = -\frac{\partial A}{\partial T}, \quad G = A + pV, \quad H = G + TS, \quad (6)$$

where p , S , G , and H are pressure, entropy, Gibbs energy, and enthalpy, respectively. The first relation obviously results in the ideal gas equation of state, $pV = RT$. The isochoric heat capacity is obtained as

$$C_v = T \frac{\partial S}{\partial T} = -T \frac{\partial^2 A}{\partial T^2}, \quad (7)$$

and the isobaric heat capacity of the ideal gas is then $C_p = C_v + R$. All these properties can be obtained using the internal partition function, Eq. (1), and its first two moments, Eqs. (2) and (3). The most important and widely used thermochemical functions can be constructed as follows:

(a) The standardized enthalpy is

$$H(T) - H(298.15) = RT \frac{Q'_{\text{int}}}{Q_{\text{int}}} + \frac{5}{2}RT - H(298.15), \quad (8)$$

where $H(298.15)$ is the (absolute) enthalpy at the reference temperature taken to be 298.15 K.

(b) The Gibbs energy function is

$$\text{gef}(T, p) = -\frac{G(T) - H(298.15)}{T} = R \ln Q_{\text{int}} + R \ln \frac{(2\pi m)^{3/2} (k_B T)^{5/2}}{h^3 p} + \frac{H(298.15)}{T}. \quad (9)$$

(c) The entropy is

$$S(T, p) = R \frac{Q'_{\text{int}}}{Q_{\text{int}}} + R \ln Q_{\text{int}} + \frac{5}{2}R + R \ln \frac{(2\pi m)^{3/2} (k_B T)^{5/2}}{h^3 p}. \quad (10)$$

(d) The isobaric heat capacity is

$$C_p(T) = R \left[\frac{Q''_{\text{int}}}{Q_{\text{int}}} - \left(\frac{Q'_{\text{int}}}{Q_{\text{int}}} \right)^2 \right] + \frac{5}{2}R. \quad (11)$$

As seen in Table 1, the physical constants used in Eqs. (1) to (11), similarly to the energy levels, have well defined uncertainties. The uncertainties of the c_2 and R constants are rather substantial, in fact larger than the relative uncertainties of many of the MARVEL energy levels. Since c_2 appears alongside the E_i energies in Eqs. (1) to (3), its uncertainty has a significant effect on the uncertainties of the computed thermochemical functions (*vide infra*).

2.5. The effect of unbound states on the thermochemical properties of water

A possible route to determine the $Q_U(T)$ contribution of the unbound rovibrational states to the partition function $Q_{\text{int}}(T)$ of water is through the use of the expression

$$Q_U(T) = \int_0^\infty \rho_U(E) \exp(-\beta E) dE, \quad (12)$$

where $\rho_U(E)$ is the density of the unbound rovibrational states for H_2^{16}O and $\beta = 1/k_B T$. In the present work, a simple model is used to evaluate Eq. (12): the unbound (scattering/continuum) states of the H_2^{16}O system are approximated as the eigenstates of the non-interacting bound OH radical and an OH + H scattering system, in which the OH is

treated as a particle with no internal degrees of freedom. The density of states for the OH radical can be given by

$$\rho^{(\text{OH})}(E) = \sum_{l,v} (2l+1) \delta(E - E_{l,v}^{(\text{OH})}), \quad (13)$$

while for the OH + H scattering system it is

$$\rho_{\text{U}}^{(\text{OH}+\text{H})}(E) = \frac{1}{\pi} \sum_j (2j+1) \frac{d\eta_j(E)}{dE}, \quad (14)$$

where l and v are the rotational and vibrational quantum numbers of the OH radical, respectively, j is the rotational quantum number of the H + OH scattering system in the center-of-mass frame, and $\eta_j(E)$ is the scattering phase shift corresponding to a given j .

Applying the formula, motivated by the probability density distribution formula for the sum of two independent random variables,

$$\rho_{\text{U}}(E) = \int_0^\infty \rho^{(\text{OH})}(E') \rho_{\text{U}}^{(\text{OH}+\text{H})}(E - E') dE', \quad (15)$$

for the total density of states, and from combining Eqs. (12), (13), (14), and (15) and utilizing the fact that $\eta_j(E)$ is zero for $E < D_0$, one obtains

$$Q_{\text{U}}(T) = \left(\sum_{l,v} (2l+1) \exp(-\beta E_{l,v}^{(\text{OH})}) \right) \left(\frac{1}{\pi} \sum_j (2j+1) \int_{D_0}^\infty \frac{d\eta_j(E')}{dE'} \exp(-\beta E') dE' \right) = Q^{(\text{OH})}(T) Q_{\text{U}}^{(\text{OH}+\text{H})}(T). \quad (16)$$

Thus, the total partition function is a product of the partition functions of the non-interacting subsystems, as expected. The final $Q_{\text{U}}(T)$ values were obtained for *ortho*- and *para*-H₂¹⁶O by multiplying the results of Eq. (16) by 3 and 1, respectively.

The potential energy curves (PEC) for the OH radical and the OH + H system were obtained from the global H₂¹⁶O PES of Refs. 56 and 61. The OH PEC was simply obtained by setting the second H to a 30 a_0 distance from the OH center-of-mass, while for the OH + H system the PEC was obtained by “relaxing” the orientation of the OH and the OH distance, within 0–3 a_0 , for each fixed OH–H distance. Eigenenergies for the OH radical in Eq. (15) were obtained by solving the diatomic rovibrational time-independent Schrödinger equation using 250 spherical-oscillator DVR basis functions⁶² with $R_{\text{max}} = 15 a_0$. As in previous studies,^{42,63} the scattering phase shifts in Eq. (14) were computed using a semi-classical WKB approximation. The maximum j value used in Eq. (14) is 278.

2.6. Uncertainty and error analysis

The exact values of the internal partition functions of molecules are unknown, and thus there are no true reference values available for comparison with the approximate values. Nev-

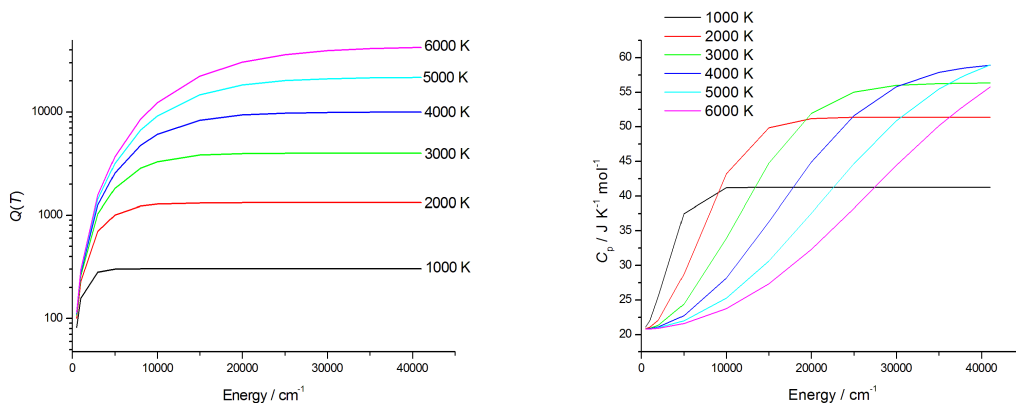


Figure 1. Left panel: Convergence of the internal partition function $Q_{\text{int}}(T)$ of H_2^{16}O at different temperatures as a function of the energy cutoff value considered in the direct sum (see text). Right panel: Similar curves for the isobaric heat capacity $C_p(T)$ of H_2^{16}O .

ertheless, in a computational study claiming high accuracy a quantification of uncertainties must be performed.⁶⁴

There are a few sources of error preventing the determination of “exact” values of $Q_{\text{int}}(T)$. Traditionally, the largest source of the uncertainty in a partition function, especially at higher temperatures, has been the uncertainty about the number of bound energy levels (uncertainty about the energy level density). A second significant source of error lies in the uncertainty of the energy levels used to determine $Q_{\text{int}}(T)$. A third type of (usually less significant) uncertainty is connected with the question of how unbound states and states associated with excited electronic states should be accounted for. A fourth source of uncertainty, so far left unexplored in computational thermochemical studies, is connected to the uncertainty of the physical constants entering Eqs. (1) through (16) (Table 1).

Checking the convergence of partition functions is very hard, since Q_{int} grows monotonically as more and more bound energy levels are considered in the direct sum. At low temperatures ($T < 1000$ K), relatively few energy levels are sufficient to reach a converged Q_{int} value (in our definition this means that adding more and more higher-lying energy levels to the sum in Eq. (1) causes only a negligible change, (much) less than 0.01 %).

Two simple methods can be used for obtaining the second type of uncertainty mentioned about the partition function and the associated thermochemical quantities: in method A the common error propagation formula can be employed, while method B increases and reduces the energy levels by their uncertainties, the two extrema of the given thermochemical function can be calculated and the difference of these extrema provides an uncertainty estimate.

The third type of uncertainty of $Q_{\text{int}}(T)$ comes from the unbound states but, to the best of our knowledge, this uncertainty has not been taken properly into account for molecules

containing more than two atoms. Part of the reason is that unbound states start playing a significant role at higher temperatures and only for molecules with a comparatively low dissociation energy. In this work, the effect of unbound states is approximated using the model described in the Sec. 2.5. In the case of bound states, where very accurate reference data are available, the accuracy of the crude “non-interacting OH plus OH+H” model for computing thermodynamic properties can be tested. In fact, this model overestimates the partition function by a factor of around four. This huge discrepancy is probably due to the fact that the model allows for quantum states with large overlaps between the hydrogen nuclei, which in a more realistic simulation would lead to very high (even unbound) energies and much smaller contributions to the partition function. The situation is expected to be similar in the case of unbound states, that is, the model defined in Sec. 2.5 is expected to overestimate the contribution of the unbound states in the partition function. Thus, taking the computed values of the contribution of unbound states themselves as the uncertainties originating from the unbound states seems to be a safe, conservative estimate.

In the present case of H_2^{16}O , the hybrid database contains all the existing bound rovibrational energy levels. Completeness of the set of hybrid energy levels may not be maintained perfectly just slightly below the first dissociation limit, where hard-to-determine long-range states may exist;^{62,65} therefore, it is worth checking the convergence of $Q_{\text{int}}(T)$ by increasing the number of energy levels considered in the direct sum via moving an E_{cut} cutoff energy value closer and closer to the dissociation limit. Figure 1 illustrates the effect of the increase of E_{cut} on the total partition sum at different temperatures. It can be seen that, while at 1000 K the partition sum is fully converged with an E_{cut} of about 8000 cm^{-1} , at 6000 K the $Q_{\text{int}}(T)$ does not reach full convergence even at $E_{\text{cut}} = D_0$, so adding new (high-lying) energy levels to the direct sum the value of the partition function might still change noticeably.

To help elucidate the results of Fig. 1, the solid lines in Fig. 2 show the difference, in %, between $Q_{\text{int}}^{\text{tot}}$ (considering all energy levels) and Q_{int}^{39000} , Q_{int}^{40000} , and Q_{int}^{41000} (*i.e.*, considering the energy levels up to $E_{\text{cut}} = 39\,000$, $40\,000$, and $41\,000\text{ cm}^{-1}$, respectively) as a function of temperature. It can be seen that (a) at 4000 K the differences are still very close to zero; and (b) at 6000 K the difference between $Q_{\text{int}}^{\text{tot}}$ and Q_{int}^{41000} is about 0.05%. The dashed lines in the left panel of Fig. 2 show the similar differences for Q_{int}'' . It can be seen that at 6000 K the error of $Q_{\text{int}}''^{41000}$ is about 0.3%. Considering that there are almost $13\,000$ energy levels between $41\,000\text{ cm}^{-1}$ and the first dissociation limit, and that this number probably grossly overestimates the number of energy levels that sophisticated first-principles computations can miss, we associate the differences of the $Q_{\text{int}}^{\text{tot}}$ and Q_{int}^{41000} values with the uncertainty which comes from the lack of a truly complete set of bound rovibronic energy levels. Figure 2 also shows why it is so important to determine all rovibrational energy levels up to the dissociation limit. At higher temperatures ($T > 3000\text{ K}$), the lack of rovibrational energy levels at the highest level density regions close to dissociation causes significant errors,

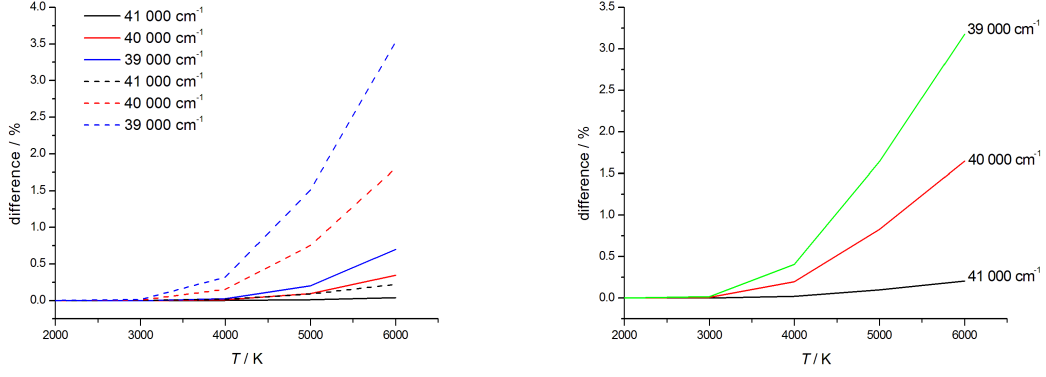


Figure 2. Left panel: Convergence characteristics of the internal partition function, $Q_{\text{int}}(T)$ (solid lines), and the second moment of $Q_{\text{int}}(T)$, $Q''_{\text{int}}(T)$ (dashed lines), of H_2^{16}O utilizing larger and larger sets of energy levels, as a function of temperature, with energy cutoff values given in the inset of the figure. Right panel: Similar curves for the isobaric heat capacity $C_p(T)$ of H_2^{16}O .

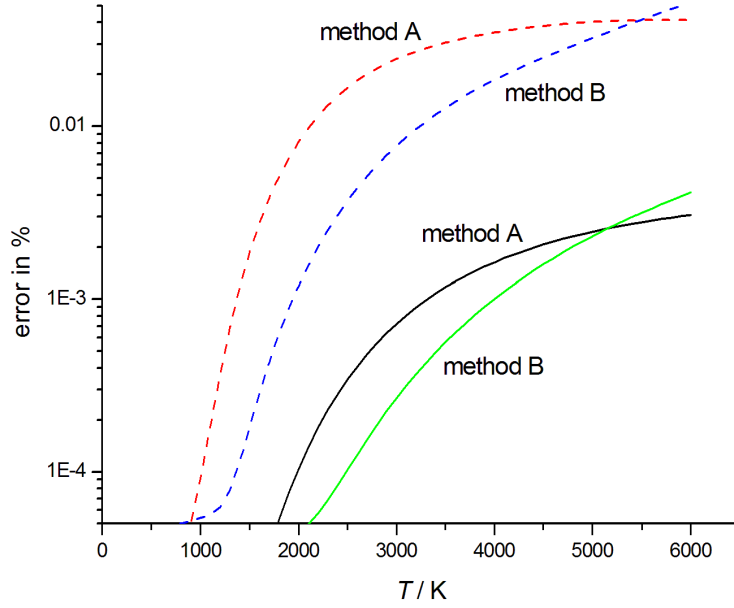


Figure 3. Error of the partition function (solid lines) and its second moment (dashed lines) using the propagation formula method, Method A, and the “two extrema” method, Method B.

especially in the cases of Q'' and C_p .

Figure 3 shows errors, in %, which come from the uncertainties of the energy levels. Most importantly, both methods A and B, see above, result in similar, relatively small errors (less than 0.004% in the case of Q_{int} and less than 0.05% in the case of Q''). C_p is the thermochemical quantity most sensitive to uncertainties of energy levels; therefore, the

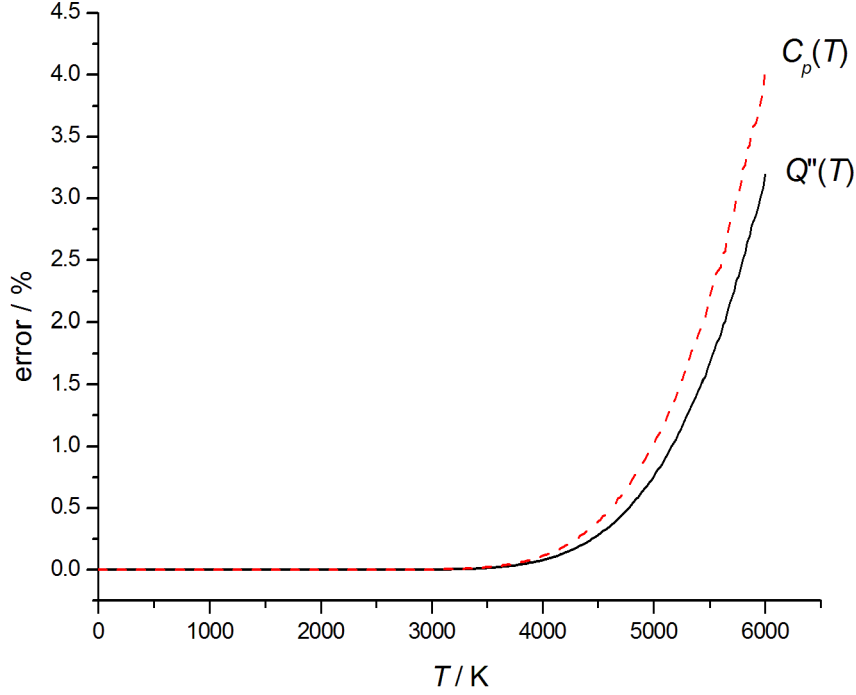


Figure 4. Error due to the neglect of the unbound states during the determination of $Q''_{\text{int}}(T)$ (solid line) and $C_p(T)$ (dashed line).

above analysis was repeated for C_p (see the right panels of Figs. 1 and 2).

Figure 4 shows the error contribution of unbound states. It can be seen that (a) up to 4000 K the contribution is very close to zero; and (b) at 6000 K the contribution is 3.2% to $Q''_{\text{int}}(T)$ and 4.0% to C_p .

There is one more source of error which might influence the final uncertainty of the partition function: the uncertainties of the physical constants. This type of uncertainty is usually negligible, for example, in case of the heat capacity the uncertainty of the molar gas constant is two orders of magnitude less than the other errors and since R is a simple scale factor its uncertainty is negligible. However, in the case of c_2 , the second radiation constant, which is the scale factor of energy levels and is inside the sum, the uncertainty of c_2 is not negligible. Figure 5 shows the effect of an assumed error of c_2 . It can be seen that below about 2500 K the uncertainty of c_2 determines the final uncertainty of the partition function. Above this temperature, the uncertainty contribution of unbound states dominates. The final uncertainty of the partition function is given by the four uncertainties just described.

Table 2. The temperature-dependent internal partition functions of *ortho*- and *para*-H₂¹⁶O, $Q_{\text{int}}^{\text{ortho}}(T)$ and $Q_{\text{int}}^{\text{para}}(T)$, respectively, and their first two moments, Q' and Q'' . The same data are also presented for the nuclear-spin-equilibrated quantity $Q_{\text{int}}(T)$. Numbers in parentheses are the approximate two standard deviation uncertainties in the last digits of the $Q_{\text{int}}(T)$, $Q'_{\text{int}}(T)$, and $Q''_{\text{int}}(T)$ data.

T/K	$Q_{\text{int}}^{\text{para}}(T)$	$Q'_{\text{int}}^{\text{para}}(T)$	$Q''_{\text{int}}^{\text{para}}(T)$	$Q_{\text{int}}^{\text{ortho}}(T)$	$Q'_{\text{int}}^{\text{ortho}}(T)$	$Q''_{\text{int}}^{\text{ortho}}(T)$	$Q_{\text{int}}(T)$	$Q'_{\text{int}}(T)$	$Q''_{\text{int}}(T)$
100	8.78855	12.79649	31.8905	26.36458	38.40031	95.5838	35.15312(6)	51.19680(5)	127.4743(1)
200	24.3538	36.0975	90.3065	73.0613	108.2926	270.9194	97.4151(1)	144.3901(1)	361.2259(3)
300	44.5301	66.5958	168.2010	133.5904	199.7875	504.603	178.1206(2)	266.3833(2)	672.8040(6)
400	68.6423	104.0492	268.974	205.9269	312.1475	806.921	274.5692(3)	416.1966(4)	1075.895(1)
500	96.5825	149.5104	399.179	289.7475	448.5312	1197.536	386.3300(4)	598.0417(6)	1596.715(2)
600	128.5401	204.4202	565.317	385.6204	613.2604	1695.952	514.1605(5)	817.6806(8)	2261.269(3)
700	164.8516	270.371	774.746	494.5548	811.114	2324.238	659.4065(6)	1081.485(1)	3098.984(4)
800	205.945	349.173	1036.321	617.835	1047.518	3108.963	823.7801(8)	1396.690(2)	4145.284(5)
900	252.325	442.889	1360.220	756.976	1328.668	4080.66	1009.301(1)	1771.558(2)	5440.879(7)
1000	304.568	553.832	1757.64	913.705	1661.495	5272.91	1218.273(1)	2215.327(3)	7030.54(1)
1100	363.316	684.527	2240.64	1089.948	2053.581	6721.91	1453.264(2)	2738.107(4)	8962.55(1)
1200	429.272	837.702	2822.18	1287.815	2513.107	8466.54	1717.087(2)	3350.809(5)	11288.73(2)
1300	503.196	1016.28	3516.21	1509.587	3048.84	10548.61	2012.783(2)	4065.120(6)	14064.82(2)
1400	585.903	1223.381	4337.74	1757.710	3670.141	13013.2	2343.613(3)	4893.522(7)	17350.94(4)
1500	678.263	1462.334	5303.00	2034.789	4387.001	15908.99	2713.052(3)	5849.335(9)	21211.99(5)
1600	781.198	1736.69	6429.52	2343.593	5210.07	19288.55	3124.790(4)	6946.76(1)	25718.07(8)
1700	895.684	2050.24	7736.2	2687.053	6150.72	23208.6	3582.737(5)	8200.96(2)	30944.8(1)
1800	1022.756	2407.02	9243.4	3068.268	7221.04	27730.1	4091.024(6)	9628.06(3)	36973.5(2)
1900	1163.504	2811.31	10973.0	3490.511	8433.94	32918.9	4654.015(7)	11245.25(4)	43891.8(3)
2000	1319.078	3267.71	12948.5	3957.232	9803.12	38845.3	5276.309(9)	13070.83(5)	51793.8(4)
2100	1490.69	3781.06	15195.0	4472.07	11343.16	45585	5962.76(1)	15124.22(7)	60780.0(6)
2200	1679.61	4356.5	17739.6	5038.84	13069.6	53218.7	6718.46(2)	17426.1(1)	70958.3(8)
2300	1887.20	4999.6	20611	5661.58	14998.7	61833	7548.78(2)	19998.3(1)	82444(1)
2400	2114.84	5716.0	23840	6344.52	17148.1	71519	8459.37(3)	22864.1(2)	95359(1)
2500	2364.04	6512.0	27459	7092.10	19536	82376	9456.14(4)	26048.0(2)	109835(2)
2600	2636.33	7394.0	31503	7908.99	22181.9	94508	10545.33(5)	29575.9(3)	126011(2)
2700	2933.36	8368.9	36009	8800.08	25106.6	108025	11733.44(6)	33475.4(4)	144034(3)
2800	3256.83	9443.9	41015	9770.49	28331.5	123045	13027.32(8)	37775.4(5)	164061(4)
2900	3608.54	10626.6	46564	10825.59	31879.7	139693	14434.12(9)	42506.3(6)	186257(5)
3000	3990.3	11925.1	52700	11971.0	35775.1	158099	15961.3(1)	47700.2(8)	210798(6)
3100	4404.2	13347.8	59467	13212.6	40043.2	178401	17616.8(1)	53391(1)	237868(9)
3200	4852.2	14904	66915	14556.5	44710	200744	19408.7(2)	59614(1)	267659(14)
3300	5336.4	16602	75094	16009.2	49805	225282	21345.6(2)	66406(2)	300376(22)
3400	5859.1	18452	84057	17577.3	55355	252171	23436.4(3)	73807(2)	336229(37)
3500	6422.6	20464	93860	19267.8	61393	281578	25690.4(3)	81857(4)	375438(60)
3600	7029.3	22649	104558	21087.9	67948	313673	28117.2(5)	90598(5)	418231(95)
3700	7681.8	25018	116211	23045.2	75055	348633	30727.0(6)	100074(9)	464844(150)
3800	8382.6	27583	128880	25147.6	82748	386639	33530.1(9)	110330(13)	515519(231)
3900	9134	30354	142626	27403	91061	427877	36538(1)	121415(20)	570503(347)
4000	9940	33344	157514	29820	100033	472541	39760(2)	133377(30)	630055(519)
4100	10803	36567	173605	32408	109700	520816	43210(3)	146266(45)	694421(751)
4200	11725	40034	190969	35175	120100	572907	46899(4)	160134(65)	763876(1081)
4300	12710	43758	209664	38130	131275	628991	50840(6)	175033(93)	838655(1507)
4400	13761	47755	229766	41284	143264	689298	55045(8)	191019(132)	919065(2103)
4500	14882	52036	251336	44645	156109	754007	59527(12)	208145(184)	1005342(2883)
4600	16075	56617	274434	48225	169851	823301	64300(17)	226468(253)	1097735(3874)
4700	17345	61512	299137	52034	184534	897411	69378(23)	246046(344)	1196548(5176)
4800	18694	66734	325519	56081	200202	976557	74775(31)	266936(462)	1302076(6882)
4900	20126	72299	353641	60379	216897	1060923	80505(42)	289196(613)	1414564(9055)
5000	21646	78222	383513	64938	234665	1150541	86584(57)	312886(806)	1534055(11566)
5100	23257	84516	415277	69769	253549	1245833	93026(75)	338066(1050)	1661110(14817)
5200	24962	91199	448970	74885	273596	1346915	99847(98)	364794(1354)	1795885(18823)
5300	26765	98283	484755	80296	294850	1454269	107062(127)	393133(1731)	1939024(24100)
5400	28672	105786	522468	86015	317357	1567409	114687(164)	423142(2195)	2089877(29895)
5500	30685	113721	562432	92054	341163	1687302	122739(209)	454884(2761)	2249734(37402)
5600	32809	122105	604338	98425	366314	1813022	131234(265)	488418(3449)	2417360(45318)
5700	35047	130952	648770	105141	392856	1946321	140188(333)	523808(4276)	2595091(55918)
5800	37405	140279	695568	112214	420837	2086714	149619(416)	561115(5267)	2782281(68522)
5900	39886	150100	744478	119657	450301	2233449	159543(515)	600401(6446)	2977927(82113)
6000	42494	160433	796005	127483	481299	2388030	169977(635)	641731(7842)	3184035(98690)

Table 3. Thermochemical functions of nuclear-spin-equilibrated H_2^{16}O . Numbers in parentheses are the approximate two standard deviation uncertainties in the last digit of the quoted value.

T/K	$C_p(T) / \text{J K}^{-1} \text{mol}^{-1}$			$S(T) / \text{J K}^{-1} \text{mol}^{-1}$			$H(T) / \text{kJ mol}^{-1}$		
	This work	Ruscic ¹⁹	VT ³⁰	This work ^a	Ruscic ¹⁹	VT ³⁰	This work	Ruscic ¹⁹	VT ³⁰
100	33.30086(1)	33.301	33.301	152.38263(7)	152.387	152.384	3.28953(1)	3.290	3.289
200	33.35053(1)	33.351	33.351	175.47984(7)	175.484	175.481	6.62199(1)	6.622	6.622
300	33.59584(1)	33.596	33.596	189.03614(7)	189.040	189.038	9.96618(1)	9.966	9.966
400	34.26208(1)	34.262	34.262	198.78271(8)	198.787	198.784	13.35574(1)	13.356	13.356
500	35.22593(1)	35.226	35.226	206.52794(8)	206.532	206.530	16.82850(1)	16.829	16.829
600	36.32471(1)	36.325	36.325	213.04616(9)	213.050	213.048	20.40529(1)	20.405	20.405
700	37.49627(1)	37.496	—	218.73282(9)	218.737	—	24.09582(1)	24.096	—
800	38.72398(1)	38.724	38.728	223.8193(1)	223.823	223.822	27.90642(1)	27.906	27.907
900	39.99172(1)	39.99	—	228.4533(1)	228.457	—	31.84196(1)	31.842	—
1000	41.27527(1)	41.269	41.287	232.7332(1)	232.737	232.737	35.90529(1)	35.905	35.907
1100	42.54776(1)	42.529	—	236.7271(1)	236.730	—	40.09664(1)	40.095	—
1200	43.78553(2)	43.739	43.809	240.4826(1)	240.482	240.490	44.41368(1)	44.409	44.419
1300	44.97088(3)	44.872	—	244.0345(1)	244.029	—	48.85199(1)	48.840	—
1400	46.09248(5)	45.909	46.124	247.4087(2)	247.393	247.420	53.40573(1)	53.380	53.417
1500	47.14441(7)	46.835	47.177	250.6250(2)	250.592	250.639	58.06816(1)	58.018	58.082
1600	48.1249(1)	—	48.157	253.6993(2)	—	253.715	62.83222(2)	—	62.850
1800	49.8780(2)	—	49.904	259.4715(4)	—	259.491	72.63700(5)	—	72.660
2000	51.3787(3)	—	51.394	264.8064(6)	—	264.828	82.7666(1)	—	82.794
2200	52.6646(4)	—	52.668	269.7651(9)	—	269.788	93.1742(2)	—	93.204
2400	53.7730(5)	—	53.766	274.396(1)	—	274.418	103.8206(3)	—	103.850
2600	54.7373(6)	—	54.724	278.739(2)	—	278.761	114.6738(4)	—	114.701
2800	55.5848(7)	—	55.571	282.827(2)	—	282.848	125.7077(5)	—	125.732
3000	56.337(1)	—	56.326	286.689(3)	—	286.708	136.9013(7)	—	136.923
3200	57.008(4)	—	57.005	290.346(4)	—	290.365	148.237(1)	—	148.257
3400	57.608(9)	—	57.614	293.821(7)	—	293.840	159.700(2)	—	159.720
3600	58.14(2)	—	58.152	297.13(1)	—	297.149	171.276(5)	—	171.298
3800	58.60(4)	—	58.613	300.28(3)	—	300.305	182.950(9)	—	182.976
4000	58.98(7)	—	58.986	303.30(5)	—	303.322	194.71(2)	—	194.737
4200	59.3(1)	—	59.259	306.19(9)	—	306.207	206.54(4)	—	206.564
4400	59.5(2)	—	59.418	308.9(2)	—	308.968	218.41(7)	—	218.433
4600	59.6(4)	—	59.451	314.1(4)	—	311.610	242.2(2)	—	230.322
4800	59.6(5)	—	59.350	315.4(5)	—	314.139	248.2(2)	—	242.205
5000	59.5(6)	—	59.111	316.6(6)	—	316.557	254.2(3)	—	254.053
5200	59.3(8)	—	58.734	318.9(9)	—	318.868	266.0(4)	—	265.840
5400	59(1)	—	58.225	321(1)	—	321.076	277.9(6)	—	277.538
5600	59(1)	—	57.591	323(2)	—	323.182	289.7(9)	—	289.122
5800	58(2)	—	56.846	325(2)	—	325.191	301(1)	—	300.567
6000	58(2)	—	56.003	327(3)	—	327.104	313(2)	—	311.854

^a The values reported in this column correspond to $S(T) - R \times \ln 4$, to make the $S(T)$ results of the present study approximately comparable to those of Refs. 19 and 30.

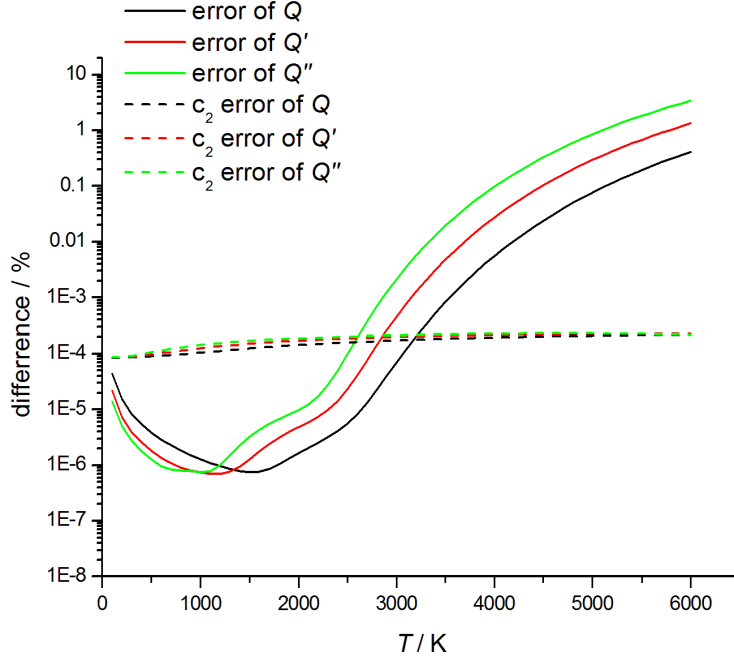


Figure 5. Error contribution of energy levels (solid lines) and the error contribution of the uncertainty of second radiation constant (dashed lines).

3. Results and Discussion

The Q , Q' , and Q'' results of *ortho*- and *para*-H₂¹⁶O, along with the nuclear-spin-equilibrated mixture, are presented in Table 2 in 100 K intervals up to 6000 K, starting at 100 K. Table 3 contains three thermochemical functions, $C_p(T)$, $S(T)$, and $H(T)$ as a function of temperature, as well as their comparison with the best previous results obtained by Ruscic¹⁹ and VT.³⁰ Note that only the traditional, nuclear-spin-equilibrated thermochemical quantities are compared with literature data in Table 3. The complete set of results at 1 K increments is given in the Supplementary Material³⁵ to this paper. Table 4 lists coefficients of a least-squares fit to our computed partition function, using the traditional form of³⁰

$$\ln Q_{\text{int}} = \sum_{i=0}^6 a_i (\ln T)^i. \quad (17)$$

In order to get the best reproduction of the directly computed values, the fit had to be performed in two separate temperature ranges. The first range is 0 – 200 K, the other is 201 – 6000 K. These fits can reproduce, in both regions, the values of $\ln Q_{\text{int}}$ reasonably accurately, within about 0.1%. Nevertheless, as emphasized, for example, by Fischer et al.,¹⁷ it is preferable these days to interpolate the tabulated thermochemical data presented in a fine grid rather than to use low-order polynomial expansions, and even a 25 K tabulation is sufficient for most partition functions.

Table 4. Coefficients of the fit, see Eq. (17), to the nuclear-spin-equilibrated internal partition function of H_2^{16}O .

Coefficient	0 – 200 K	201 – 6000 K
a_0	0.0000414145	86.9112357472
a_1	5.2668268683	-60.7285954830
a_2	-8.4438709824	15.4447694151
a_3	4.9777150504	-1.3899526096
a_4	-1.3449867842	-0.0424069070
a_5	0.1743063797	0.0143520410
a_6	-0.0087936229	-0.0006287480

3.1. The partition function

What the dimensionless partition function tells us is basically the ratio of the total number of “particles” to the number of “particles” in the ground state. Thus, the partition function provides a greatly simplified measure of how the particles are partitioned among the available energy levels. The magnitude of the partition function depends upon the magnitude of the fractional populations, and the latter depend both on the relative energy of the state and the chosen temperature. The largest value of the partition function can be very large but not infinite if the system contains a finite number of “particles”. As seen in Table 2, $Q_{\text{int}}(T)$ of H_2^{16}O becomes large as the temperature increases, reaching about (1, 1200, 5300, 16 000, 40 000, 87 000, 170 000) at temperatures of (0, 1000, 2000, 3000, 4000, 5000, 6000) K.

3.2. Comparison with previous results

The simplest way to approximate the partition function is through the application of the rigid-rotor and harmonic-oscillator (RRHO) model. For the RRHO model an analytical formula is known for generating the partition function. Using experimental spectroscopic constants ($A = 835\,839.9$ MHz, $B = 435\,354.5$ MHz, and $C = 278\,133.3$ MHz from Ref. 66; $\nu_1 = 3657.053251$ cm^{-1} , $\nu_2 = 1594.746292$ cm^{-1} , and $\nu_3 = 3755.928548$ cm^{-1} from Ref. 48), the temperature-dependent internal partition function can easily be computed. Figure 6 shows the differences for $Q_{\text{int}}(T)$ and $C_p(T)$ between the “exact” values of this study and those of the “analytical” RRHO partition function. Although the difference between the exact and the RRHO values can be significant for $Q_{\text{int}}(T)$, especially at higher temperatures, considering the extreme simplicity of this model the agreement observed is quite pleasing for this semirigid molecule. Note also that most of the difference between the discrete, “exact” results and the continuous, “analytical” RRHO results at the lowest temperatures, below about 350 K, is due to failure of the integration approximation. The differences would tend toward zero if the experimental spectroscopic constants reported were used to

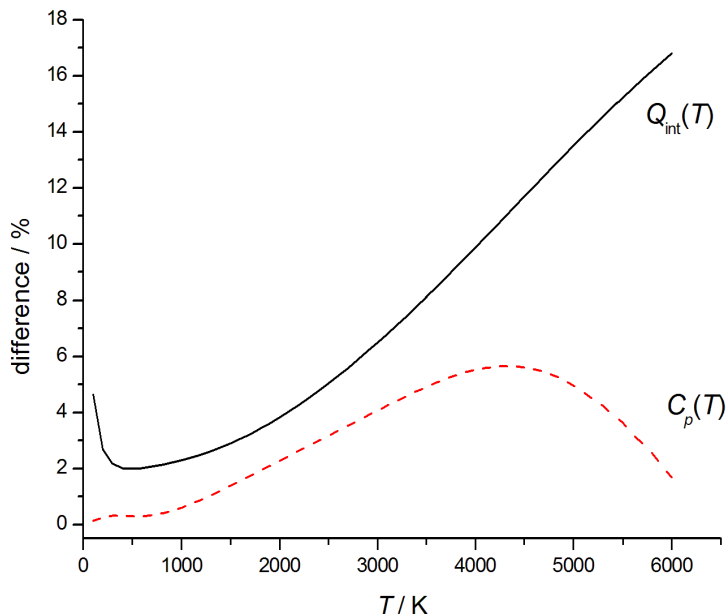


Figure 6. Percentage difference between the “exact” values of $Q_{\text{int}}(T)$ and $C_p(T)$ and those corresponding to the “analytical” rigid-rotor-harmonic-oscillator (RRHO) approximation. The apparent increase in the differences below 350 K for $Q_{\text{int}}(T)$ is due to the failure of approximating the direct sum with an integral when the density of states is low.

generate rovibrational energy levels and these were used, via direct summation, for the computation of $Q_{\text{int}}(T)$. Note that, in a relative sense, the RRHO approximation works seemingly considerably better for $C_p(T)$ than for $Q_{\text{int}}(T)$.

The left panel of Fig. 7 shows the comparison of our internal partition function with other high-temperature values by Harris *et al.*,²⁹ Irwin,⁶⁷ and VT.³⁰ The agreement with the VT results is especially pleasing. The right panel of Fig. 7 compares our $C_p(T)$ values with those of Harris *et al.*,⁶⁵ JANAF,¹⁵ and VT.³⁰ As expected, the deviations here are slightly larger, but VT works very well below 4500 K.

3.3. NASA polynomials

The tabular form of thermochemical data used to be not very convenient for computerized applications. Thus, more than four decades ago Gordon and McBride⁶⁸ suggested a set of low-order polynomials providing a convenient set of fit functions known as the older 7-constant and the newer 9-constant NASA polynomials. As Ruscic *et al.*⁶⁹ emphasized, (a) the 9-constant NASA polynomial reproduces the underlying data about two orders of magnitude better than the 7-constant NASA polynomial, and (b) the thermochemical properties can be calculated in general with confidence in the fourth and fifth digit in the range of 150–3000 K. Nevertheless, the accuracy of even the 9-constant NASA polynomial is clearly insufficient

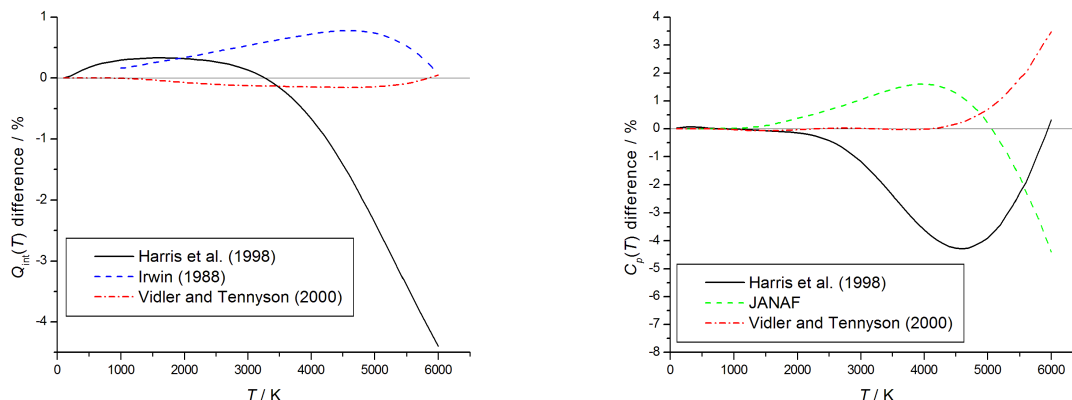


Figure 7. Left panel: Comparison of the present $Q_{\text{int}}(T)$ values with those of Harris *et al.*,²⁹ Irwin,⁶⁶ and Vidler and Tennyson.³⁰ Right panel: Comparison of the present $C_p(T)$ values with those of Harris *et al.*,²⁹ JANAF,¹⁵ and Vidler and Tennyson.³⁰

when the data of the present study are considered. Therefore, thermochemical quantities determined in this study are provided in the Supplementary Material³⁵ at 1 K intervals. For those who need highly accurate thermochemical data, it is recommended to adapt the tabulated functions.

3.4. CODATA

The outstanding accuracy of the experimental (MARVEL) energy levels employed in this study means that all thermochemical quantities computed, especially at lower temperatures, have exceedingly high accuracy (the list of MARVEL rovibrational energies is complete up to 7500 cm^{-1}). One such quantity is $H^\circ(298.15\text{ K}) - H^\circ(0\text{ K})$, the standard molar enthalpy increment (standard integrated heat capacity) of H_2^{16}O between 298.15 and 0 K ($H^\circ(0\text{ K}) = 0.0\text{ J mol}^{-1}$). This value is given for water in the official CODATA compilation¹⁰ as $9.905 \pm 0.005\text{ kJ mol}^{-1}$. Naturally, the value we compute, $9.90404 \pm 0.00001\text{ kJ mol}^{-1}$, falls within the limits of the old value, but it is more accurate by about two orders of magnitude. The newly determined value is insensitive to any reasonable change in the energy levels; the value is completely determined by energy levels lower than about 5000 cm^{-1} , and, notably, even the present first-principles PoKaZaTeL energy levels yield the same value though with higher uncertainty. While the present suggested change in the standard molar enthalpy increment of H_2^{16}O is more or less inconsequential for most of thermochemistry, as enthalpies of formation cannot be determined with this exceedingly small uncertainty, it nevertheless exemplifies the fact that it is more and more realistic to use high-resolution spectroscopic data to directly calculate thermodynamic quantities with minuscule uncertainties.

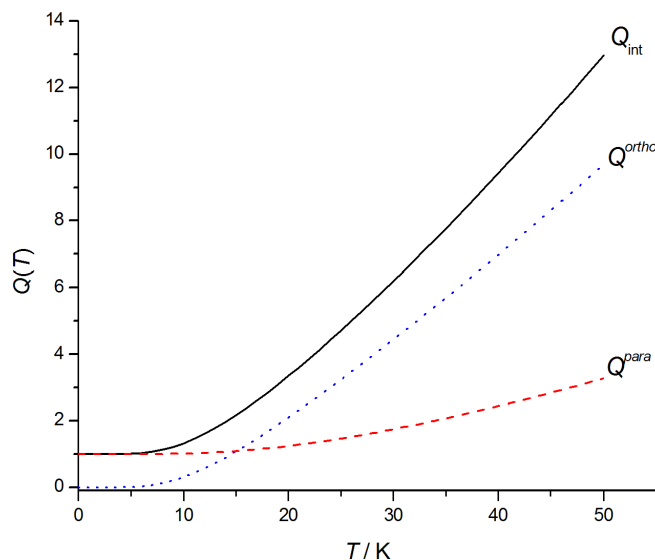


Figure 8. The *ortho*-H₂¹⁶O (dotted, blue curve), the *para*-H₂¹⁶O (dashed, red curve), and the nuclear-spin-equilibrated H₂¹⁶O (full, black curve) partition functions at low temperatures, below 50 K.

3.5. The low-temperature limit

Standard thermochemical textbooks and standard thermochemical tables found in various compendia^{11,15} venture very rarely below 100 K. The reason is that there are special considerations about partition functions as well as thermochemical functions at the lowest temperatures, (well) below 100 K, due to the effect of nuclear spin statistics. It is only for higher temperatures that the *ortho* and *para* spin isomers of water are equilibrated, while in thermochemistry one always assumes an equilibrated mixture. In fact, the effect of nuclear spins can be investigated on effective structural parameters, as has been done for H₂O⁷⁰ and NH₃.⁷¹ Due to the distinct rovibrational states, the *ortho* and *para* species have slightly different effective structures and different thermochemical functions. The two nuclear-spin isomers can be in equilibrium (note again that this is what we always assume in thermochemistry), or, if their interconversion is kinetically hindered, they exist as a mixture corresponding to distinct nuclear spin temperatures.^{72,73} The same phenomenon is well known and has been studied^{74,75} at the dawn of quantum mechanics for the H₂ molecule.

Figure 8 shows the values of the internal partition functions of the *ortho* and *para* spin isomers of H₂¹⁶O below 50 K. The different low-temperature behavior of $Q_{\text{int}}^{\text{ortho}}$ and $Q_{\text{int}}^{\text{para}}$ is evident from the figure. As mentioned, it is only the nuclear-spin-equilibrated $Q_{\text{int}}(T)$ which is part of traditional thermochemistry. The reader should also be warned that one should not mix thermochemical data adhering to different definitions, in this case the convention used to represent whether nuclear spin effects are considered or not.

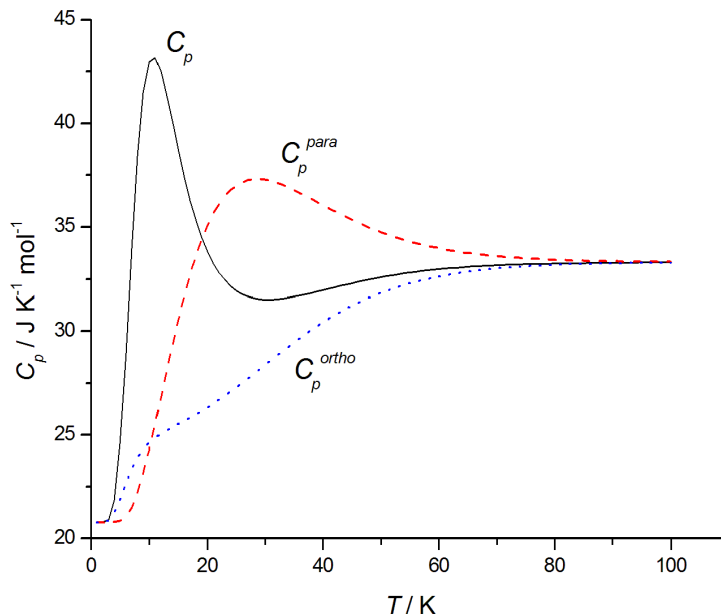


Figure 9. The *ortho*-H₂¹⁶O (dotted, blue curve), the *para*-H₂¹⁶O (dashed, red curve), and the nuclear-spin-equilibrated H₂¹⁶O (full, black curve) isobaric heat capacities at low temperatures, below 100 K.

Figure 9 shows the isobaric heat capacity of the *ortho* and *para* spin isomers as a function of temperature, as well as that of the equilibrium mixture. It is seen that up to 80 K the two water isomers possess rather different curves, but above 100 K the two curves become basically the same.

It must also be noted that the ortho-to-para (OPR) ratio is a useful diagnostic tool in astrochemistry.⁷⁶ The drastically different isobaric heat capacity of *ortho*- and *para*-H₂¹⁶O between 10 K and 60 K computed here with high accuracy may have important consequences for certain applications.

4. Summary and Conclusions

The ideal-gas internal partition functions determined in this study for *ortho*-H₂O, *para*-H₂O, and their nuclear-spin-equilibrated mixture, in the temperature range of 0–6000 K, are the most accurate ones produced to date. The partition functions as well as the subsequently determined thermochemical functions, including the standardized enthalpy, the entropy, and the isobaric heat capacity, have their own temperature-dependent uncertainties. All these thermochemical quantities are listed in 100 K increments in the main text and in 1 K increments in the Supplementary Material;³⁵ the latter should support several modeling applications. The accuracy of the present data is due to the following characteristics of this

study:

(1) The internal partition function $Q_{\text{int}}(T)$ and its first two moments are determined via the explicit summation technique; thus, their determination involves no modeling assumptions beyond the bare basics, distinguishing this study from almost all previous efforts.

(2) A large number of highly accurate, experimental rovibrational energy levels determined previously⁴⁸ are utilized; the list of experimental levels is complete up to 7500 cm^{-1} , significantly lowering the uncertainty of $Q_{\text{int}}(T)$ below about 1000 K.

(3) At higher temperatures, between about 1000 K and 3000 K, the completeness of the energy level set determines the true accuracy of the thermochemical quantities determined. We utilized the complete set of bound rovibrational energy levels of H_2^{16}O obtained from a first-principles variational nuclear motion computation involving an exact kinetic energy operator and a highly accurate empirical PES.³⁶ Altogether close to one million bound energy levels are utilized in this study.

(4) In order to ensure accuracy between 3000 and 6000 K, the contribution due to unbound states is considered via a simple model computation. Our test computations show that for H_2^{16}O the contribution from the excited electronic states can be safely neglected.

Although in this study highly accurate thermochemical functions have been obtained for *ortho*- and *para*- H_2^{16}O , it is not yet common to include nuclear-spin statistical factors in the computation of partition functions and the related thermochemical functions. Thus, these data should be used with caution in chemical reactions where nuclear spin effects are neglected for the other species involved. Nevertheless, it is expected that such data, especially important at low temperatures, will become available for a growing number of chemical species.

The accuracy of the reproduction of the present data with the 7- and 9-constant NASA polynomials is orders of magnitude worse than the internal accuracy of our results. Thus, it is recommended to use the 1 K list of computed values in all applications requiring high accuracy.

It is recommended that the new, exceedingly accurate value of the standard molar enthalpy increment (integrated heat capacity) of H_2^{16}O , $H^\circ(298.15\text{ K}) = 9.90404(1)\text{ kJ mol}^{-1}$, should replace the value advocated in the CODATA compilation,¹⁰ $9.905 \pm 0.005\text{ kJ mol}^{-1}$.

Finally, we note that the present procedure and data serve well the mission of IAPWS to determine accurate ideal- and real-gas data for water. For this task we need similarly high-quality data for all water isotopologues present in Vienna Standard Mean Ocean Water (VSMOW),^{77–79} providing the isotopic composition⁷⁸ of so-called “ordinary water substance.” Work in this direction is in progress.

Acknowledgments

The authors are grateful to the COST action “Molecules in Motion” (MOLIM, CM1405) for support. AGC thanks the NKFIH (grant number NK83583 and K119658) for supporting the work performed in Hungary. JH acknowledges support provided by the Czech Science Foundation (grant no. 16-02647S). The authors are indebted to Professors Roberto Marquardt and Branko Ruscic for their useful comments on certain aspects of this study.

References

- ¹P. F. Bernath, *Phys. Chem. Chem. Phys.* **4**, 1501 (2002).
- ²N. F. Zobov, S. V. Shirin, R. I. Ovsyannikov, O. L. Polyansky, R. J. Barber, J. Tennyson, P.-F. Coheur, P. F. Bernath, M. Carleer, and R. Colin, *Mon. Not. Royal Astron. Soc.* **387**, 1093 (2008).
- ³O. L. Polyansky, N. F. Zobov, I. I. Mizus, L. Lodi, S. N. Yurchenko, J. Tennyson, A. G. Császár, and O. V. Boyarkin, *Phil. Trans. Royal Soc. London A* **370**, 2728 (2012).
- ⁴D. L. Baulch, C. J. Cobos, R. A. Cox, P. Frank, G. Hayman, T. Just, J. A. Kerr, T. Murrells, M. J. Pilling, J. Troe, R. W. Walker, and J. Warnatz, *J. Phys. Chem. Ref. Data* **23**, 847 (1994).
- ⁵A. Burcat, *Third millennium ideal gas and condensed phase thermochemical database for combustion, TAE Report No. 867* (Technion, Haifa, 2001).
- ⁶G. N. Lewis, M. Randall, K. S. Pitzer, and L. Brewer, *Thermodynamics* (McGraw-Hill, New York, 1961).
- ⁷J. D. Cox, *Pure Appl. Chem.* **54**, 1239 (1982).
- ⁸D. F. McMillan and D. M. Golden, *Annu. Rev. Phys. Chem.* **33**, 493 (1982).
- ⁹M. W. Chase, C. A. Davies, J. R. Downey, Jr., D. A. Frurip, R. A. McDonald, and A. N. Syverud, *J. Phys. Chem. Ref. Data* **14**, 1 (1985).
- ¹⁰J. D. Cox, D. D. Wagman, and V. A. Medvedev, *CODATA Key Values for Thermodynamics* (Hemisphere, New York, 1989).
- ¹¹L. V. Gurvich, I. V. Veyts, and C. B. Alcock, *Thermodynamic Properties of Individual Substances* (Hemisphere, New York, 1989).
- ¹²J. B. Pedley, *Thermochemical data and structures of organic compounds, Vol. 1* (Thermodynamics Research Center, College Station, TX, 1994).
- ¹³J. Berkowitz, G. B. Ellison, and D. Gutman, *J. Phys. Chem.* **98**, 2744 (1994).
- ¹⁴W. Wagner, J. R. Cooper, A. Dittmann, J. Kijima, H. Kretzschmar, A. Kruse, R. Mares, K. Oguchi, H. Sato, I. Stocker, O. Sifner, Y. Takaishi, I. Tanishita, J. Trubenbach, and T. Willkommen, *J. Eng. Gas Turbines Power* **122**, 150 (2000).
- ¹⁵M. W. Chase, *J. Phys. Chem. Ref. Data Monograph No. 9*, 1 (1998).
- ¹⁶W. Wagner and A. Pruß, *J. Phys. Chem. Ref. Data* **31**, 387 (2002).

- ¹⁷J. Fischer, R. R. Gamache, A. Goldman, L. S. Rothman, and A. Perrin, *J. Quant. Spectrosc. Radiat. Transfer* **82**, 401 (2003).
- ¹⁸J. Tennyson, S. N. Yurchenko, A. F. Al-Refaie, E. J. Barton, K. L. Chubb, P. A. Coles, S. Diamantopoulou, M. N. Gorman, C. Hill, A. Z. Lam, L. Lodi, L. K. McKemmish, Y. Na, A. Owens, O. L. Polyansky, T. Rivlin, C. Sousa-Silva, D. S. Underwood, A. Yachmenev, and E. Zak, *J. Mol. Spectrosc.* **372**, 73 (2016).
- ¹⁹B. Ruscic, *J. Phys. Chem. A* **117**, 11940 (2013).
- ²⁰J. E. Mayer and M. G. Mayer, *Statistical Mechanics* (Wiley, New York, 1940).
- ²¹D. A. McQuarrie, *Statistical Mechanics* (University Science Books, Sausalito, 2000).
- ²²A. F. Krupnov, *Phys. Rev. A* **82**, 036703 (2010).
- ²³K. K. Irikura, *Essential Statistical Thermodynamics* (American Chemical Society, Washington, DC, 1998).
- ²⁴A. L. L. East and L. Radom, *J. Chem. Phys.* **106**, 6655 (1997).
- ²⁵R. B. McClurg, R. C. Flagan, and W. A. Goddard III, *J. Chem. Phys.* **106**, 6675 (1997).
- ²⁶P. Y. Ayala and H. B. Schlegel, *J. Chem. Phys.* **108**, 2314 (1998).
- ²⁷O. L. Polyansky, A. G. Császár, S. V. Shirin, N. F. Zobov, P. Barletta, J. Tennyson, D. W. Schwenke, and P. J. Knowles, *Science* **299**, 539 (2003).
- ²⁸J. M. L. Martin, J. P. Francois, and R. Gijbels, *J. Chem. Phys.* **96**, 7633 (1992).
- ²⁹G. J. Harris, S. Viti, H. Y. Mussa, and J. Tennyson, *J. Chem. Phys.* **109**, 7197 (1998).
- ³⁰M. Vidler and J. Tennyson, *J. Chem. Phys.* **113**, 9766 (2000).
- ³¹C. C. Stephenson and H. O. McMahon, *J. Chem. Phys.* **7**, 614 (1939).
- ³²R. Q. Topper, Q. Zhang, Y. P. Liu, and D. G. Truhlar, *J. Chem. Phys.* **98**, 4991 (1993).
- ³³F. V. Prudente and A. J. C. Varandas, *J. Phys. Chem. A* **106**, 6193 (2002).
- ³⁴L. Gurvich, I. V. Veyts, C. B. Alcock, and V. S. Iorish, *Thermodynamic Properties Of Individual Substances: Elements and Compounds*, 4th ed. in 5 vols. (Hemisphere, New York, 1991).
- ³⁵“See supplementary material at [url to be inserted] for listings of various temperature-dependent thermochemical quantities, both with and without estimated contributions for unbound states,” (2016).
- ³⁶O. L. Polyansky, A. A. Kyuberis, N. Zobov, J. Tennyson, L. Lodi, and S. N. Yurchenko, *Mon. Not. Roy. Astron. Soc.* (2016).
- ³⁷R. J. Barber, J. Tennyson, G. J. Harris, and R. N. Tolchenov, *Mon. Not. Royal Astron. Soc.* **368**, 1087 (2006).
- ³⁸J. Tennyson, N. F. Zobov, R. Williamson, O. L. Polyansky, and P. F. Bernath, *J. Phys. Chem. Ref. Data* **30**, 735 (2001).
- ³⁹S. Viti, J. Tennyson, and O. L. Polyansky, *Mon. Not. Royal Astron. Soc.* **287**, 79 (1997).
- ⁴⁰S. Viti, *Infrared spectra of cool stars and sunspots*, Ph.D. thesis, University of London (1997).

- ⁴¹H. Y. Mussa and J. Tennyson, J. Chem. Phys. **109**, 10885 (1998).
- ⁴²T. Szidarovszky and A. G. Császár, J. Chem. Phys. **142**, 014103 (2015).
- ⁴³N. F. Zobov, S. V. Shirin, L. Lodi, B. C. Silva, J. Tennyson, A. G. Császár, and O. L. Polyansky, Chem. Phys. Lett. **507**, 48 (2011).
- ⁴⁴T. Szidarovszky and A. G. Császár, Mol. Phys. **111**, 2131 (2013).
- ⁴⁵A. G. Császár, G. Czakó, T. Furtenbacher, and E. Mátyus, Ann. Rep. Comp. Chem. **3**, 155 (2007).
- ⁴⁶T. Furtenbacher, A. G. Császár, and J. Tennyson, J. Mol. Spectrosc. **245**, 115 (2007).
- ⁴⁷T. Furtenbacher and A. G. Császár, J. Quant. Spectrosc. Radiat. Transfer **113**, 929 (2012).
- ⁴⁸J. Tennyson, P. F. Bernath, L. R. Brown, A. Campargue, M. R. Carleer, A. G. Császár, L. Daumont, R. R. Gamache, J. T. Hodges, O. V. Naumenko, O. L. Polyansky, L. S. Rothman, A. C. Vandaele, N. F. Zobov, A. R. Al Derzi, C. Fábri, A. Z. Fazliev, T. Furtenbacher, I. E. Gordon, L. Lodi, and I. I. Mizus, J. Quant. Spectrosc. Radiat. Transfer **117**, 29 (2013).
- ⁴⁹J. Tennyson, P. F. Bernath, L. R. Brown, A. Campargue, M. R. Carleer, A. G. Császár, R. R. Gamache, J. T. Hodges, A. Jenouvrier, O. V. Naumenko, O. L. Polyansky, L. S. Rothman, R. A. Toth, A. C. Vandaele, N. F. Zobov, L. Daumont, A. Z. Fazliev, T. Furtenbacher, I. E. Gordon, S. N. Mikhailenko, and S. V. Shirin, J. Quant. Spectrosc. Radiat. Transfer **110**, 573 (2009).
- ⁵⁰J. Tennyson, P. F. Bernath, L. R. Brown, A. Campargue, M. R. Carleer, A. G. Császár, L. Daumont, R. R. Gamache, J. T. Hodges, O. V. Naumenko, O. L. Polyansky, L. S. Rothman, R. A. Toth, A. C. Vandaele, N. F. Zobov, A. Z. Fazliev, T. Furtenbacher, I. E. Gordon, S. N. Mikhailenko, and B. A. Voronin, J. Quant. Spectrosc. Radiat. Transfer **111**, 2160 (2010).
- ⁵¹J. Tennyson, P. F. Bernath, L. R. Brown, A. Campargue, A. G. Császár, L. Daumont, R. R. Gamache, J. T. Hodges, O. V. Naumenko, O. L. Polyansky, L. S. Rothman, A. C. Vandaele, N. F. Zobov, N. Dénes, A. Z. Fazliev, T. Furtenbacher, I. E. Gordon, S.-M. Hu, T. Szidarovszky, and I. A. Vasilenko, J. Quant. Spectrosc. Radiat. Transfer **142**, 93 (2014).
- ⁵²J. Tennyson, P. F. Bernath, L. R. Brown, A. Campargue, A. G. Császár, L. Daumont, R. R. Gamache, J. T. Hodges, O. V. Naumenko, O. L. Polyansky, L. S. Rothman, A. C. Vandaele, and N. F. Zobov, Pure Appl. Chem. **86**, 71 (2014).
- ⁵³A. G. Császár and T. Furtenbacher, J. Mol. Spectrosc. **266**, 99 (2011).
- ⁵⁴H. W. Kroto, *Molecular Rotation Spectra* (Dover, New York, 1992).
- ⁵⁵A. G. Császár, C. Fábri, T. Szidarovszky, E. Mátyus, T. Furtenbacher, and G. Czakó, Phys. Chem. Chem. Phys. **13**, 1085 (2012).
- ⁵⁶O. L. Polyansky, A. G. Császár, S. V. Shirin, N. F. Zobov, P. Barletta, J. Tennyson, D. W. Schwenke, and P. J. Knowles, Science **299**, 539 (2003).

- ⁵⁷J. Tennyson, M. A. Kostin, P. Barletta, G. J. Harris, O. L. Polyansky, J. Ramanlal, and N. F. Zobov, *Chem. Phys. Chem.* **163**, 85 (2004).
- ⁵⁸O. V. Boyarkin, M. A. Koshelev, O. Aseev, P. Maksyutenko, T. R. Rizzo, N. F. Zobov, L. Lodi, J. Tennyson, and O. L. Polyansky, *Chem. Phys. Lett.* **568-569**, 14 (2013).
- ⁵⁹P. J. Mohr, D. B. Newell, and B. N. Taylor, *Rev. Mod. Phys.* **88**, 035009 (2016).
- ⁶⁰“<http://www.ciaaw.org/>,” (2016).
- ⁶¹P. Barletta, S. V. Shirin, N. F. Zobov, O. L. Polyansky, J. Tennyson, E. F. Valeev, and A. G. Császár, *J. Chem. Phys.* **125**, 204307 (2006).
- ⁶²T. Szidarovszky, A. G. Császár, and G. Czakó, *Phys. Chem. Chem. Phys.* **12**, 8373 (2010).
- ⁶³F. H. Mies and P. S. Julienne, *J. Chem. Phys.* **77**, 6162 (1982).
- ⁶⁴H. Chung, B. J. Braams, K. Bartschat, A. G. Császár, G. Drake, T. Kirchner, V. Kokoouline, and J. Tennyson, *J. Phys. D: Appl. Phys.* **49**, 363002 (2016).
- ⁶⁵J. J. Munro, J. Ramanlal, and J. Tennyson, *New J. Phys.* **7**, 196 (2005).
- ⁶⁶A. G. Császár, G. Czakó, T. Furtenbacher, J. Tennyson, V. Szalay, S. V. Shirin, N. F. Zobov, and O. L. Polyansky, *J. Chem. Phys.* **122**, 214305 (2005).
- ⁶⁷A. W. Irwin, *Astron. Astrophys., Suppl. Ser.* **74**, 145 (1988).
- ⁶⁸B. J. McBride and S. Gordon, *Computer Program for Calculating and Fitting Thermodynamic Functions* (NASA RP-1271, 1992).
- ⁶⁹B. Ruscic, J. E. Boggs, A. Burcat, A. G. Császár, J. Demaison, R. Janoschek, J. M. L. Martin, M. L. Morton, M. J. Rossi, J. F. Stanton, P. G. Szalay, P. R. Westmoreland, F. Zabel, and T. Bérces, *J. Phys. Chem. Ref. Data* **34**, 573 (2005).
- ⁷⁰G. Czakó, E. Mátyus, and A. G. Császár, *J. Phys. Chem. A* **113**, 11665 (2009).
- ⁷¹I. Szabó, C. Fábri, G. Czakó, E. Mátyus, and A. G. Császár, *J. Phys. Chem. A* **116**, 4356 (2012).
- ⁷²N. Dello Russo, M. A. DiSanti, K. Magee-Sauer, E. L. Gibb, M. J. Mumma, R. J. Barber, and J. Tennyson, *Icarus* **168**, 186 (2004).
- ⁷³N. Dello Russo, B. P. Bonev, M. A. DiSanti, E. L. Gibb, M. J. Mumma, K. Magee-Sauer, R. J. Barber, and J. Tennyson, *Astrophys. J.* **621**, 537 (2005).
- ⁷⁴D. M. Dennison, *Proc. Roy. Soc. A* **115**, 483 (1927).
- ⁷⁵K. F. Bonhoeffer and P. Harteck, *Z. Physikal. Chem.* **4B**, 113 (1929).
- ⁷⁶K. Furuya, Y. Aikawa, U. Hincelin, G. E. Hassel, E. A. Bergin, A. I. Vasyunin, and E. Herbst, *Astron. Astrophys.* **584**, A124 (2015).
- ⁷⁷R. Gonfiantini, *Nature* **271**, 534 (1978).
- ⁷⁸National Institute of Standards and Technology, “Report of Investigation, Reference Materials 8535, 8535a,” (2005).
- ⁷⁹National Institute of Standards and Technology, “Report of Investigation, Reference Material 8535a,” (2011).

